1-1-2014

Fluid flow shear stress over podocytes is increased in the solitary kidney.

Tarak Srivastava
Children's Mercy Hospital

Gianni E. Celsi

Mukut Sharma

Hongying Dai
Children's Mercy Hospital

Ellen T. McCarthy

See next page for additional authors

Nephrol Dial Transplant (2014) 29: 65–72
doi: 10.1093/ndt/gft387
Advance Access publication 28 October 2013

Fluid flow shear stress over podocytes is increased in the solitary kidney

Tarak Srivastava[1],
Gianni E. Celsi[2],
Mukut Sharma[3],
Hongying Dai[1],
Ellen T. McCarthy[4],
Melanie Ruiz[1],
Patricia A. Cudmore[1],
Uri S. Alon[1],
Ram Sharma[3]
and Virginia A. Savin[3]

[1]Section of Nephrology, Children's Mercy Hospital and University of Missouri at Kansas City, Kansas City, MO, USA,
[2]Uppsala University Hospital, Uppsala, Sweden,
[3]Research and Development, Kansas City VA Medical Center, Kansas City, MO, USA and
[4]Kidney Institute, University of Kansas Medical Center, Kansas City, MO, USA

Correspondence and offprint requests to: Tarak Srivastava; E-mail: tsrivastava@cmh.edu

Keywords: fluid flow shear stress, glomerular hyperfiltration, podocyte, solitary kidney

ORIGINAL ARTICLE

ABSTRACT

Background. Glomerular hyperfiltration is emerging as the key risk factor for progression of chronic kidney disease (CKD). Podocytes are exposed to fluid flow shear stress (FFSS) caused by the flow of ultrafiltrate within Bowman's space. The mechanism of hyperfiltration-induced podocyte injury is not clear. We postulated that glomerular hyperfiltration in solitary kidney increases FFSS over podocytes.

Methods. Infant Sprague–Dawley rats at 5 days of age and C57BL/6J 14-week-old adult mice underwent unilateral nephrectomy. Micropuncture and morphological studies were then performed on 20- and 60-day-old rats. FFSS over podocytes in uninephrectomized rats and mice was calculated using the recently published equation by Friedrich *et al.* which includes the variables—single nephron glomerular filtration rate (SNGFR), filtration fraction (f), glomerular tuft diameter ($2R_T$) and width of Bowman's space (s).

Results. Glomerular hypertrophy was observed in uninephrectomized rats and mice. Uninephrectomized rats on Day 20 showed a 2.0-fold increase in SNGFR, 1.0-fold increase in $2R_T$ and 2.1-fold increase in FFSS, and on Day 60 showed a 1.9-fold increase in SNGFR, 1.3-fold increase in $2R_T$ and 1.5-fold increase in FFSS, at all values of modeled 's'. Similarly, uninephrectomized mice showed a 2- to 3-fold increase in FFSS at all values of modeled SNGFR.

Conclusions. FFSS over podocytes is increased in solitary kidneys in both infant rats and adult mice. This increase is a consequence of increased SNGFR. We speculate that increased FFSS caused by reduced nephron number contributes to podocyte injury and promotes the progression of CKD.

INTRODUCTION

Congenital anomalies of the kidney and urinary tract (CAKUT) constitute the most common cause of chronic kidney disease (CKD) in children. In contrast to traditionally held views, children born with a solitary kidney are currently considered to be at risk for progressive renal injury [1, 2]. Sanna-Cherchi *et al.* [1] found that ~50% of children born with solitary kidney progress to end-stage renal disease as young adults. Glomerular hyperfiltration is emerging as the key risk factor for progression in CKD in children with solitary kidneys since the classical risk factors of hypertension and proteinuria do not manifest until late puberty [1–5]. A reduction in nephron number results in adaptive changes in glomerular physiology. Hemodynamic changes include increased renal blood flow (RBF) and increased glomerular capillary pressure

(P_{GC}) that results in increased single nephron glomerular filtration rate (SNGFR). In addition, glomerular hypertrophy leads to increased glomerular tuft area. These hemodynamic and structural changes contribute to glomerular injury, continuation of nephron loss and progression of CKD [6–9].

Intra-capillary pressure in the glomerulus (in the range of 60 mmHg in humans) leads to tensile stress, resulting in capillary wall stretch. The flow of ultrafiltrate within Bowman's space causes shear stress. Thus, podocytes are exposed to mechanical forces of stretch (tensile stress) transmitted by tension on the capillary wall and fluid flow shear stress (FFSS) imposed by the flow of ultrafiltrate through Bowman's space, recently reviewed by Endlich and Endlich [10]. Podocytes are the primary target for hyperfiltration-mediated injury. *In vitro* studies of stretch and FFSS show that podocytes respond to both of these stimuli [11–14]. Computational analysis of changes in cytoskeleton, cytoplasm, nucleus and membrane components shows that effects of FFSS are more pronounced on cellular compartments compared with those transmitted by cellular stretch [15]. Cultured podocytes are highly sensitive to FFSS [10]. We have shown that podocytes respond to FFSS by up-regulation of cyclooxygenase-2 enzyme protein, an elevated levels of prostaglandin E_2 and increased expression of prostanoid receptor EP2 [14, 16]. These effects of FFSS are distinct from the previously reported effects of stretch over podocytes *in vitro* [17–20].

We postulated that glomerular hyperfiltration, in conditions characterized by reduced nephron number, leads to increased FFSS over podocytes. In turn, FFSS contributes to podocyte injury and promote the progression of CKD. Direct measurement of FFSS in intact kidney is not feasible. Presently, we addressed this hypothesis by applying a mathematical model proposed by Friedrich *et al.* [13] to calculate FFSS over podocytes. We analyzed (i) micropuncture data obtained in rats that were uninephrectomized during the neonatal period [21, 22] and (ii) morphometric data obtained after unilateral nephrectomy in adult mice. We found that calculated FFSS over podocytes is increased in both model of reduced nephron number.

MATERIALS AND METHODS

Mathematical model for calculating the FFSS over podocytes

The FFSS encountered by podocyte *in vivo* in the present studies using uninephrectomized rats and mice was calculated using a method described by Friedrich *et al.* [13]. The mathematical equation described by these investigators to estimate FFSS on the surface of podocytes during filtration was based on a simplified glomerular geometry in which the glomerular tuft was represented by a sphere separated from a spherical Bowman's capsule by the distance '*s*'. '*s*' is the distance between the podocyte surface and the surface of glomerular parietal epithelial cells lining the Bowman's capsule [10]. Briefly, the FFSS (τ) over podocyte is a function of viscosity of the glomerular ultrafiltrate (η), filtration fraction (f), SNGFR, glomerular tuft diameter ($2R_T$), width of the Bowman's space (s) and of the position between the vascular and urinary poles (z)

$$\tau = \frac{3\eta \times f \times \mathrm{SNGFR}}{\pi \times s^2 \times (s + 2R_T)} \times \frac{z}{\sqrt{z \times (1-z)}}$$

Friedrich *et al.* estimated the FFSS (τ) over podocyte surface in a healthy adult mouse to be ~0.3 dyn/cm^2. This calculation was based on estimations of viscosity ($\eta = 1$ centipoise), filtration fraction ($f = 0.2$), SNGFR (SNGFR = 12 nL/min), tuft diameter ($R_T = 50$ μm) and three assumed values for '*s*' at various points between the vascular and urinary poles. These equations have not been applied to determine the likely effect of shear stress on podocytes following a reduction in renal mass *in vivo*.

Rat solitary kidney model

We have previously described the effects of renal mass reduction in 20- and 60-day-old rats that were uninephrectomized on Day 5 after birth. We used direct micropuncture and morphological [21, 22] data to calculate FFSS over podocytes in a solitary kidney. Briefly, right unilateral nephrectomy or sham operation was performed in 5-day-old male Sprague–Dawley rats. Animals were then returned to dams. At ages 20 and 60 days, rats were anesthetized, intubated and jugular vein and carotid artery were cannulated. Clearance of polyfructosan-S (Inutest) and p-aminohippuric acid were used to determine GFR and renal plasma flow. One hour before the experiments, rats were given an intravenous bolus dose of 8% Inutest at 1 mL/100 g body weight in isotonic saline followed by a continuous infusion of 8% Inutest at 1 mL/100 g body weight/hour. Three to six samples of superficial proximal tubular fluid were collected in 1–3 min with a sharpened glass capillary tube. A blood sample was also obtained at the end of the clearance period. The morphological measurements for glomerular tuft diameters were performed on the first five superficial glomeruli examined in a series of 1 μm thick sections beginning at the surface of the kidney. The largest diameter of the glomerular tuft and its perpendicular were measured, and the mean value was reported as the final glomerular tuft diameter. The measurements for f, SNGFR and $2R_T$ are shown in Table 1. The shear stress (τ) over podocyte was calculated using three separate models of '*s*' as described by Friedrich *et al.* [13]. The values used for developing the models for '*s*' were: (i) $s = 6$ μm, (ii) s increases linearly from $s = 2$ μm (at $z = 0$, the vascular pole) to 8 μm (at $z = 1$, the urinary pole) and (iii) s increases linearly from 3 μm (at $z = 0$) to 10 μm (at $z = 1$).

Mouse solitary kidney model

The width of Bowman's space '*s*' is not easily available in published literature. We carried out unilateral nephrectomy in mice with the intent to measure the width of Bowman's space '*s*'. Left nephrectomy was performed on eight adult (four males and four females) C57BL/6J mice at 14 weeks of age and kidneys were saved. Mice were sacrificed after 2 weeks ($n = 4$ males) or 3 weeks ($n = 4$ females). Right kidneys were harvested at the end of the experiment. Kidneys were fixed in 10% formalin, embedded in paraffin, sectioned at 3–5 μm and stained using Jones silver stain. The images were

Table 1. Values for SNGFR, tuft diameter ($2R_T$) and filtration fraction (f) adapted from Celsi *et al.* [21, 22] for calculating FFSS over rat podocytes at 20 and 60 days following unilateral nephrectomy at 5 days of age

Sprague–Dawley rat	SNGFR	$2R_T$	f
Control Day 20	7.4 ± 0.7	63.6 ± 0.8	0.32
Unilateral nephrectomy Day 20	15.0 ± 1.5	65.2 ± 2.4	0.34
Control Day 60	43.5 ± 3.2	102.2 ± 2.8	0.32
Unilateral nephrectomy Day 60	80.7 ± 4.6	136.8 ± 4.9	0.34

obtained using Olympus BX60 (Hamburg, Germany) for light microscopy, and analyzed by computerized image analysis using Analysis™ software. The measurements of the right kidney were compared with the paired control left kidney removed at the onset of the experiment.

Glomerular tuft area (G_A), Bowman's area (B_A), glomerular diameter (G_D or $2R_T$), Bowman's space diameter (B_D) and the width of Bowman's space (s) for 30 glomeruli from 20 superficial and 10 deep nephrons were calculated. The measurements were made on the first 10 superficial and 5 deep glomeruli from the upper pole to mid-pole, and repeated for the lower pole to mid-pole for each paired kidney. Maximal G_D and B_D were measured and the difference between the maximal G_D and B_D gave the first value for 'S_{MAX}'. We then measured 's' at six additional points at 45°, 90°, 135° drawn from the line measuring the maximal G_D. A schematic diagram illustrates the various parameters measured during morphometry procedure for each individual glomerulus (Figure 1). Thus, a total of 7 measurements of 's' per glomerulus or 210 measurements/kidney were obtained. These were averaged (S_{AVG}) for each kidney. The FFSS over podocytes *in vivo* was then modeled for the expected change in FFSS for incremental increases in SNGFR from 10 to 100%. Calculations were based on measured values for the glomerular tuft diameter ($2R_T$) and the width of Bowman's space (s) using both S_{MAX} and S_{AVG}. Student's paired t-test was used and a P-value of <0.05 was considered significant. These studies were carried out using protocols approved by the Institutional Animal Care and Use Committee (IACUC), Safety Subcommittee and the R&D Committee at the VA Medical Center, Kansas City, MO, USA.

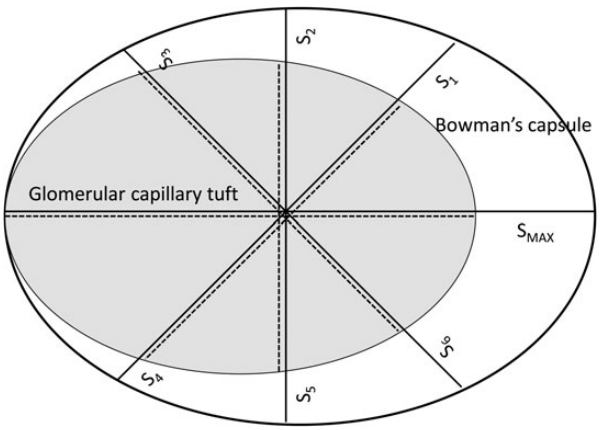

FIGURE 1: Schematic diagram illustrating the method followed during the morphometry to determine glomerular capillary tuft diameter (G_D), Bowman's space diameter (B_D) and width of Bowman space (s) of individual glomeruli. Maximal G_D and B_D were measured and the difference between the maximal G_D and B_D yielded 'S_{MAX}'. Bowman space 's' was then measured at six additional points at lines drawn at 45°, 90°, 135° from the line measuring the S_{MAX}. Thus, a total of seven measurements of 's' per glomerulus were made and then averaged (S_{AVG}) for each glomerulus. Glomerular diameter (G_D) is shown by broken/dashed lines and Bowman's space diameter (B_D) by solid lines.

RESULTS

Rat solitary kidney model

Figure 2 shows that FFSS increases with age in both uninephrectomized and sham-treated rats. The calculated FFSS using three separate model values of 's' are shown in Figure 2 and Supplementary Table S1. Models for 's' were as follows: (i) 6 µm, (ii) linearly increasing 's' from $s = 2$ µm (at $z = 0$) to 8 µm (at $z = 1$) and (iii) linearly increasing 's' from $s = 3$ µm (at $z = 0$) to 10 µm (at $z = 1$). FFSS in uninephrectomized rats was significantly higher than in sham-treated controls over a range of SNGFR, $2R_T$ and 'f' using each of the three models.

The age-related increase in FFSS was significant in both control and uninephrectomized groups. The calculated FFSS in solitary kidney is increased ~2-fold and ~1.5-fold at 20- and 60-day-old rats, respectively (Figure 2 and Supplementary Table S1). Table 1 shows that SNGFR in control animals increased from 7.4 ± 0.7 to 43.5 ± 3.2 nL/min (5.9-fold) between 20 and 60 days of age while $2R_T$ changed from 63.6 ± 0.8 to 102.2 ± 2.8 µm (1.6-fold). Similarly, SNGFR in the uninephrectomized animals increased from 15.0 ± 1.5 to 80.7 ± 4.6 nL/min (5.4-fold) from 20 to 60 days; $2R_T$ in these animals increased from 65.2 ± 2.4 to 136.8 ± 4.9 µm (2.1-fold) at 20 and 60 days. Unilateral nephrectomy increased SNGFR by 2.0- and 1.9-fold at 20 and 60 days and increased $2R_T$ by 1.0- and 1.3-fold at 20 and 60 days, respectively (Table 1) [21, 22]. Thus, although the glomerular tuft diameter in uninephrectomized animals increases by 60 days, it does not appear to prevent the change in FFSS caused by increased SNGFR.

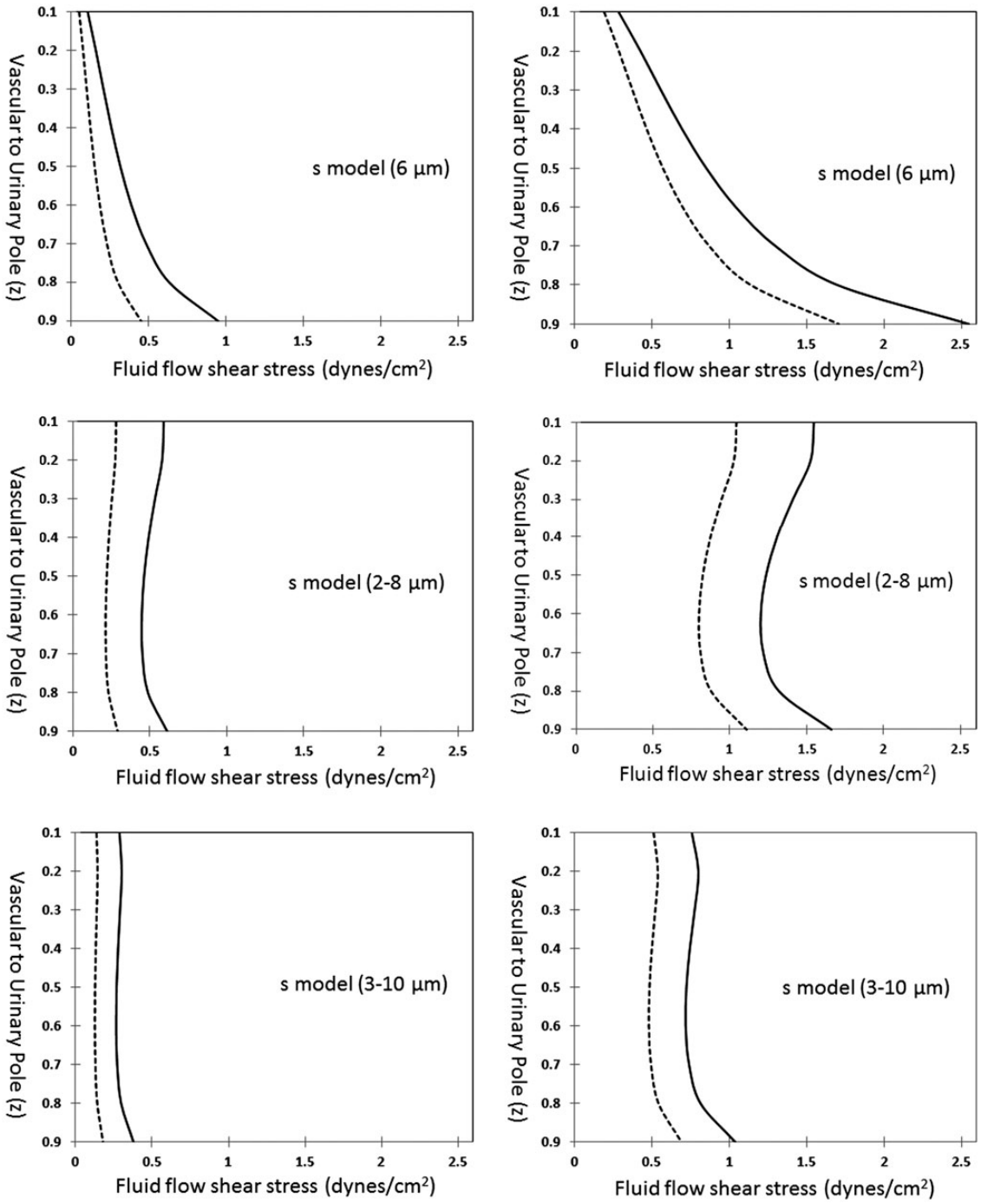

FIGURE 2: The calculated FFSS (dynes/cm^2) over podocytes in 20-day-old rats (left panel) and in 60-day-old rats (right panel) following unilateral nephrectomy at 5 days of age were modeled using the equation $\tau = 3\eta \times f \times \text{SNGFR}/(\pi \times s^2 \times (s + 2R_T)) \times (z/\sqrt{z \times (1 - z)})$ at different values of '*s*': (**a**) model $s = 6$ µm (upper row), (**b**) model of linearly increasing '*s*' from $s = 2$ µm (at $z = 0$) to 8 µm (at $z = 1$) (middle row) and (**c**) model of linearly increasing '*s*' from $s = 3$ µm (at $z = 0$) to 10 µm (at $z = 1$) (bottom row). Each line represents the FFSS curve with the mean values for SNGFR and $2R_T$. The hatched lines represent sham control rats and solid lines represent rats following unilateral nephrectomy. Curves are parallel but shifted to the right following uninephrectomy.

Additional calculations for FFSS at ±1 SD and ±2 SD for measured SNGFR and $2R_T$ resulted in nine data sets. The lowest calculated FFSS (−2 SD for SNGFR and +2 SD for $2R_T$) and the highest calculated FFSS (+2 SD for SNGFR and −2 SD for $2R_T$) on mathematical modeling for the three different values of '*s*' for 20- and 60-day-old rats are shown in Supplementary Table S1. There was no overlap between calculated FFSS in control and uninphrectomized rats (Supplementary Table S1). The increase in FFSS over podocytes in rats with solitary kidney is seen with all three modeled values of '*s*' for the measured values of SNGFR, $2R_T$ and f (Figure 2).

Table 2. The calculated fold change in FFSS following unilateral left nephrectomy in mice modeled at 10% incremental increase in SNGFR from 10 to 100% using measured mean values for $2R_T$, S_{MAX} and S_{AVG} value

	Incremental increase in SNGFR over control									
Fold change in FFSS in solitary kidney	10%	20%	30%	40%	50%	60%	70%	80%	90%	100%
Mean S_{MAX} value	1.47	1.60	1.74	1.87	2.00	2.14	2.27	2.40	2.54	2.67
Mean S_{AVG} value	2.00	2.18	2.37	2.55	2.73	2.91	3.09	3.28	3.46	3.64

Mouse solitary kidney model

The quantitative morphometric measurements obtained using eight mice were pooled for analysis. The solitary right kidney at 2–3 weeks weighed significantly more than the control left kidney (216.8 ± 42.5 versus 199.4 ± 28.3 mg, P = 0.033, $n = 8$ in each group). As expected, unilateral nephrectomy resulted in a significant increase in G_A (2.5 ± 0.8 versus 3.1 ± 1.0 × 10^3 μm^2, P ≤ 0.001), B_A (2.9 ± 0.9 versus 3.4 ± 1.2 × 10^3 μm^2, P ≤ 0.001), G_D or $2R_T$ (59.6 ± 9.6 versus 65.4 ± 11.0 μm, P ≤ 0.001) and B_D (62.5 ± 9.9 versus 68.0 ± 11.4 μm, P ≤ 0.001), but resulted in decreased S_{MAX} (2.9 ± 1.0 versus 2.6 ± 1.1 μm, P = 0.12) and S_{AVG} (2.0 ± 0.5 versus 1.6 ± 0.6 μm, P ≤ 0.001). We calculated the relative increase in FFSS at increments in SNGFR ranging from 10 to 100% compared with control values. Table 2 shows the increase in FFSS based on the measured values for $2R_T$ and S_{MAX} and S_{AVG}. Results indicate that FFSS over podocytes in the mouse is increased after unilateral nephrectomy. Changes in FFSS in the four male mice at 2 weeks and four female mice at 3 weeks following left nephrectomy were comparable (data for subset analysis not shown). We calculated the increase in FFSS over podocytes in solitary mouse kidney based on the measured G_D ($2R_T$), S_{MAX} and S_{AVG} with the assumption that filtration fraction 'f' was not significantly changed following unilateral nephrectomy. This assumption would lead to, if any, an underestimation of FFSS over podocytes in a solitary kidney. The increase in SNGFR in published literature varies based on the animal strain and experimental conditions studied with minimum of 30% and maximum of 86% [21–25].

DISCUSSION

Congenital or acquired reduction in renal mass is associated with hyperfiltration that permits maintenance of normal or nearly normal total GFR. Hyperfiltration appears to be adaptive as it preserves GFR and permits control of plasma volume and composition. However, persistent hyperfiltration results in glomerulosclerosis, albuminuria/proteinuria and progressive azotemia [6–9]. In children born with solitary kidneys, we assume that increased P_{GC} and SNGFR are present at birth, while albuminuria and proteinuria do not appear until pubertal years [1, 2]. The absence of hypertension and proteinuria during childhood also supports the concept that glomerular hyperfiltration plays an essential role in the initiation and progression of CKD [1, 2]. Since CAKUT remains the most common cause of childhood CKD and since CKD may progress to ESRD in young adults, studies aimed at understanding the injury from glomerular hyperfiltration in children are likely to provide key insights into progression of CKD [1, 2]. Mouse and rat models of renal mass reduction such as 5/6 nephrectomy or unilateral nephrectomy provide well-established techniques to study both acute and long-term effects of glomerular dysfunction induced by hyperfiltration [24–33].

Experimental reduction in nephron number results in adaptive responses that involve changes in a number of physiological parameters. Among these the rise in RBF and increased P_{GC} are responsible for initiation and maintenance of high SNGFR. Glomerular size, measured as tuft diameter in histological sections or as filtration area estimated from morphometric analyses, increases over time. The net result of these changes is a continued increase in SNGFR, despite decreased hydraulic permeability [21, 22]. During hyperfiltration, podocytes are exposed to increased mechanical stretch (tensile stress) resulting from increased capillary pressure. Dilated capillaries coupled with increased P_{GC} lead to increased wall tension and stretching of podocyte foot processes. Previous studies to understand the role of increased mechanical stretch during hyperfiltration do not fully explain podocyte injury [10–12, 17–20, 34–37]. These studies suggest involvement of the actin/integrin system, angiotensin II-mediated signaling through Type 1 angiotensin II receptors (AT1R), Erk1/2 and Akt pathways or COX-2/EP4-mediated p38 MAPK signaling. In addition to increased mechanical stretch, podocytes are exposed to increased FFSS generated by the flow of ultrafiltrate within the urinary space [13, 14, 16]. The glomerular ultrafiltrate reaches the proximal tubule via the (i) inter-podocyte space, (ii) sub-podocyte space or (iii) peripheral urinary space. The sub-podocyte space is believed to cover almost half of the glomerular filtration surface. Such segmental distribution of flow also implies that specific cellular structures may be responsible for sensing mechanical forces to intracellular components. We propose that FFSS is mainly sensed through primary processes and the soma of podocytes from ultrafiltrate flow into the sub-podocyte space and inter-podocyte space, respectively. Secondary processes that form filtration slit around the capillary loop are likely responsible for sensing the substrate stretch caused by increased intra-capillary pressure. Thus, FFSS may influence podocyte structure more

significantly than heretofore recognized and it may be the principal mediator of hyperfiltration-induced glomerular changes.

The effects of substrate stretch and FFSS have been studied extensively in osteocytes that are essential for maintaining bone integrity. Excessive generation of FFSS due to flow of intraosseous fluid during weight bearing can cause osteocytes damage. Studies suggest that FFSS causes greater cellular morphology and deformation of intracellular compartments compared with substrate stretch applied to cultured osteocytes [15]. Application of FFSS to osteocytes increases the expression of COX-2 and PGE2 receptor EP2 but not EP4, and activates GSK-3β/β-catenin and PKA signaling pathways [38–42]. We have used the information regarding osteocyte as a backdrop for designing and interpreting our initial studies on the effects of FFSS on cultured podocytes [14, 16].

With a long-term aim to understand the mechanistic basis of FFSS-mediated glomerular injury, we showed that FFSS causes increased synthesis and secretion of prostaglandin E_2 and up-regulation of prostanoid receptor EP2 in cultured podocytes [14, 16]. Similarly, Friedrich *et al.* [13] showed that FFSS activates specific tyrosine kinases that play a role in actin cytoskeleton reorganization in podocytes. These observations are based on *in vitro* experimental settings and needed to be followed up to ascertain a meaningful increase in FFSS using *in vivo* model(s) of hyperfiltration. Since a direct measurement of FFSS is not feasible, we used mathematical modeling to compute the changes in FFSS in two models of glomerular hyperfiltration. The mathematical model used to generate the equation used in the present work makes certain assumptions that include a spherical glomerular tuft and Bowman's capsule separated by a distance '*s*' with a homogenous exit of the filtrate and a laminar flow. The equation was applied to calculate FFSS using experimental data from podocytes cultured *in vitro* and from an *in vivo* model of Anti-Thy1.1 glomerulonephritis in rats [13]. This equation has not been tested previously in animal models of hyperfiltration. Validation of this equation would permit estimation of the magnitude of FFSS between experimental groups provided the underlying assumptions of homogenous exit of filtrate and a laminar flow remain comparable.

We studied kidneys after uninephrectomy in two different animal species, and calculated the FFSS over podocytes. FFSS was increased in both rat and mouse models. In rats, glomerular changes at 20 and 60 days after unilateral nephrectomy were evaluated to determine temporal changes following uninephrectomy as well as during maturation. Rats underwent unilateral nephrectomy at 5 days of age by which time nephrogenesis in rat is complete; thus, the reduction in nephron number was induced at a stage comparable with the time of birth in humans with a solitary kidney. By Days 20 and 60, the calculated FFSS was increased 1.5- to 2-fold compared with control (Figure 2). The limitation of using historical micropuncture data was that Bowman's space (*s*) was not measured simultaneously. Therefore, we analyzed FFSS using '*s*' values previously used to arrive at the equation for a mathematical model [13]. We further addressed this constraint by direct measurement of the width of Bowman's space '*s*' in uninephrectomized C57BL/6J mice.

Uninephrectomy in the adult mice resulted in a significant increase in kidney weight. Increased glomerular diameter confirmed glomerular hypertrophy. Additionally, morphometric analysis revealed increased glomerular area in histologic sections. As in rats, morphometric analysis of mouse glomeruli also showed increased FFSS. Because SNGFR and filtration fraction were not directly measured, calculations for FFSS required estimation of these parameters. Our assumption that filtration fraction remained constant is supported by the finding that direct determination of SNGFR in rats following uninephrectomy showed only a marginal increase in filtration fraction (Table 1). Additionally, increased filtration fraction would only lead to a further increase in FFSS and strengthen this postulate.

The magnitude of the increase in SNGFR after uninephrectomy in various rodent models ranges widely. Reported values are 30 and 36% in db/db and C67BL/6J mice, and 57, 57–67% and 73–86% in spontaneously hypertensive, WKY and Sprague–Dawley rats [21–25]. Therefore, we calculated FFSS using 10–100% incremental rise in SNGFR to include a wide range. In a model based on a conservative 20–40% increase in SNGFR, the FFSS on mouse podocytes would increase by 1.5- to 2.5-fold following uninephrectomy compared with controls (Table 2).

We measured '*s*' in mouse kidneys that is subject to tissue fixation artifacts and may not reflect the absolute true measurement of Bowman's space *in vivo*. Ideally, direct *in vivo* measurement of '*s*' should obviate the artifacts induced by tissue processing. Two-photon intravital microscopy (2-photon microscopy) offers direct observation of individual glomeruli in live animals. However, data acquisition in this *in vivo* imaging technique is based on distribution of fluorescent markers in various glomerular compartments. Review of published glomerular images from 2-photon microscopy studies showed that defining clear boundaries between Bowman's capsule and glomerular capillary may be subject to errors. Also, pulse-induced movement in the animal will further compromise precise measurements. The calculated FFSS using 2-photon technique maybe lower if the *in vivo* Bowman's space is wider or vice-versa compared with the values obtained using the present technique. Thus, 2-photon microscopy would impose limitations on the data due to unique features of this technology. Another potential limitation in our current approach to analyze FFSS *in vivo* is that in the present mathematical model, glomerular tuft of capillaries is represented as a single sphere, and does not take into consideration difference between podocytes located in inner and outer capillary loops within the glomeruli. However, we believe these subtle aspects of glomerular function will become clearer with a better understanding of sub-podocyte and inter-podocyte spaces and their influence on filtration and flow.

We also observed that physiological FFSS over podocytes increases with age (Figure 2) in both control and uninephrectomized rats, an anticipated effect of changes in SNGFR and G_D with age (Table 1). One could argue that the increase in G_D, i.e. glomerular hypertrophy, would attenuate FFSS from the associated rise in SNGFR. Also, despite using the ±2 SD

for $2R_T$ and SNGFR in rats, we failed to see an overlap in the calculated FFSS in all the three model values of '*s*' used (Supplementary Table S1). These results suggest that the increase in FFSS following reduction in nephron number is independent of age. It increased to a comparable degree in both infant rat and adult mouse models. Glomerular hypertrophy did not offset the increase in FFSS.

In summary, we used a mathematical model to calculate FFSS over podocytes in models of solitary kidney. Our data indicate that glomerular hyperfiltration is associated with markedly increased FFSS over podocytes after uninephrectomy both in adult mice and in young rats. Studies to understand the cellular mechanisms underlying hyperfiltration-mediated podocyte injury are essential to explaining the mechanisms of development and progression of CKD. We believe that understanding and targeting hyperfiltration-mediated injury will be valuable in developing interventions to slow the progression of CKD in both adults and children.

SUPPLEMENTARY DATA

Supplementary data are available online at http://ndt.oxfordjournals.org.

ACKNOWLEDGEMENTS

This work was supported in part by The Norman S. Coplon Extramural Research Grant and The Sam and Helen Kaplan Research Fund in Pediatric Nephrology (Srivastava, Alon). Partial support from grants from NIH: R01 DK 43752 and DK R21 00292588 (V.A.S.), DK 1RO1 DK064969 (E.T.M.) and from the VA BX001037 (V.A.S.) and funds from the Midwest Biomedical Research Foundation (V.A.S., R.S.).

CONFLICT OF INTEREST STATEMENT

None declared.

REFERENCES

1. Sanna-Cherchi S, Ravani P, Corbani V *et al.* Renal outcome in patients with congenital anomalies of the kidney and urinary tract. Kidney Int 2009; 76: 528–533
2. Westland R, Schreuder MF, Bökenkamp A *et al.* Renal injury in children with a solitary functioning kidney—the KIMONO study. Nephrol Dial Transplant 2011; 26: 1533–1541
3. Schreuder MF, Langemeijer ME, Bökenkamp A *et al.* Hypertension and microalbuminuria in children with congenital solitary kidneys. J Paediatr Child Health 2008; 44: 363–368
4. Argueso LR, Ritchey ML, Boyle ET, Jr *et al.* Prognosis of patients with unilateral renal agenesis. Pediatr Nephrol 1992; 6: 412–416
5. Argueso LR, Ritchey ML, Boyle ET, Jr *et al.* Prognosis of children with solitary kidney after unilateral nephrectomy. J Urol 1992; 148: 747–751
6. Brenner BM. Nephron adaptation to renal injury or ablation. Am J Physiol 1985; 249: F324–F337
7. Brenner BM, Mackenzie HS. Nephron mass as a risk factor for progression of renal disease. Kidney Int Suppl 1997; 63: S124–S127
8. Brenner BM, Lawler EV, Mackenzie HS. The hyperfiltration theory: a paradigm shift in nephrology. Kidney Int 1996; 49: 1774–1777
9. Neuringer JR, Brenner BM. Hemodynamic theory of progressive renal disease: a 10-year update in brief review. Am J Kidney Dis 1993; 22: 98–104
10. Endlich N, Endlich K. The challenge and response of podocytes to glomerular hypertension. Semin Nephrol 2012; 32: 327–341
11. Durvasula RV, Petermann AT, Hiromura K *et al.* Activation of a local tissue angiotensin system in podocytes by mechanical strain. Kidney Int 2004; 65: 30–39
12. Endlich N, Kress KR, Reiser J *et al.* Podocytes respond to mechanical stress in vitro. J Am Soc Nephrol 2001; 12: 413–422
13. Friedrich C, Endlich N, Kriz W *et al.* Podocytes are sensitive to fluid shear stress in vitro. Am J Physiol Renal Physiol 2006; 291: F856–F865
14. Srivastava T, McCarthy ET, Sharma R *et al.* Prostaglandin E_2 is crucial in the podocytes response to fluid flow shear stress. J Cell Commun Signal 2010; 4: 79–90
15. McGarry JG, Klein-Nulend J, Mullender MG *et al.* A comparison of strain and fluid shear stress in stimulating bone cell responses—a computational and experimental study. FASEB J 2005; 19: 482–484
16. Srivastava T, McCarthy ET, Sharma R *et al.* Fluid flow shear stress upregulates prostanoid receptor EP2 but not EP4 in murine podocytes. Prostaglandins Other Lipid Mediat 2012, doi:10.1016/j.prostaglandins.2012.11.001
17. Martineau LC, McVeigh LI, Jasmin BJ *et al.* p38 MAP kinase mediates mechanically induced COX-2 and PG EP4 receptor expression in podocytes: implications for the actin cytoskeleton. Am J Physiol Renal Physiol 2004; 286: F693–F701
18. Faour WH, Thibodeau JF, Kennedy CR. Mechanical stretch and prostaglandin E2 modulate critical signaling pathways in mouse podocytes. Cell Signal 2010; 22: 1222–1230
19. Stitt-Cavanagh EM, Faour WH, Takami K *et al.* A maladaptive role for EP4 receptors in podocytes. J Am Soc Nephrol 2010; 21: 1678–1690
20. Faour WH, Gomi K, Kennedy CR. PGE(2) induces COX-2 expression in podocytes via the EP4 receptor through a PKA-independent mechanism. Cell Signal 2008; 20: 2156–2164
21. Celsi G, Savin J, Henter JI *et al.* The contribution of ultrafiltration pressure for glomerular hyperfiltration in young nephrectomized rats. Acta Physiol Scand 1991; 141: 483–487
22. Celsi G, Larsson L, Seri I *et al.* Glomerular adaptation in uninephrectomized young rats. Pediatr Nephrol 1989; 3: 280–285
23. Levine DZ, Iacovitti M, Robertson SJ *et al.* Modulation of single-nephron GFR in the db/db mouse model of type 2 diabetes mellitus. Am J Physiol Regul Integr Comp Physiol 2006; 290: R975–R981
24. Bank N, Alterman L, Aynedjian HS. Selective deep nephron hyperfiltration in uninephrectomized spontaneously hypertensive rats. Kidney Int 1983; 24: 185–191
25. Hayslett JP, Kashgarian M, Epstein FH. Mechanism of change in the excretion of sodium per nephron when renal mass is reduced. J Clin Invest 1969; 48: 1002–1006

26. Wang JL, Cheng HF, Shappell S *et al.* A selective cyclooxygenase-2 inhibitor decreases proteinuria and retards progressive renal injury in rats. Kidney Int 2000; 57: 2334–2342
27. Hostetter TH, Olson JL, Rennke HG *et al.* Hyperfiltration in remnant nephrons: a potentially adverse response to renal ablation. Am J Physiol 1981; 241: F85–F93
28. Olson JL, Hostetter TH, Rennke HG *et al.* Altered glomerular permselectivity and progressive sclerosis following extreme ablation of renal mass. Kidney Int 1982; 22: 112–126
29. Kren S, Hostetter TH. The course of the remnant kidney model in mice. Kidney Int 1999; 56: 333–337
30. Flyvbjerg A, Schrijvers BF, De Vriese AS *et al.* Compensatory glomerular growth after unilateral nephrectomy is VEGF dependent. Am J Physiol Endocrinol Metab 2002; 283: E362–E366
31. Nath KA, Chmielewski DH, Hostetter TH. Regulatory role of prostanoids in glomerular microcirculation of remnant nephrons. Am J Physiol 1987; 252: F829–F837
32. Wang JL, Cheng HF, Zhang MZ *et al.* Selective increase of cyclooxygenase-2 expression in a model of renal ablation. Am J Physiol 1998; 275: F613–F622
33. Stahl RA, Kudelka S, Paravicini M *et al.* Prostaglandin and thromboxane formation in glomeruli from rats with reduced renal mass. Nephron 1986; 42: 252–257
34. Petermann AT, Pippin J, Durvasula R *et al.* Mechanical stretch induces podocyte hypertrophy in vitro. Kidney Int 2005; 67: 157–166
35. Schordan S, Schordan E, Endlich K *et al.* AlphaV-integrins mediate the mechanoprotective action of osteopontin in podocytes. Am J Physiol Renal Physiol 2011; 300: F119–F132
36. Miceli I, Burt D, Tarabra E *et al.* Stretch reduces nephrin expression via an angiotensin II-AT(1)-dependent mechanism in human podocytes: effect of rosiglitazone. Am J Physiol Renal Physiol 2010; 298: F381–F390
37. Dessapt C, Baradez MO, Hayward A *et al.* Mechanical forces and TGFbeta1 reduce podocyte adhesion through α3β1 integrin downregulation. Nephrol Dial Transplant 2009; 24: 2645–2655
38. Kamel MA, Picconi JL, Lara-Castillo N *et al.* Activation of β-catenin signaling in MLO-Y4 osteocytic cells versus 2T3 osteoblastic cells by fluid flow shear stress and PGE2: implications for the study of mechanosensation in bone. Bone 2010; 47: 872–881
39. Kitase Y, Barragan L, Qing H *et al.* Mechanical induction of PGE2 in osteocytes blocks glucocorticoid-induced apoptosis through both the β-catenin and PKA pathways. J Bone Miner Res 2010; 25: 2657–2668
40. Xia X, Batra N, Shi Q *et al.* Prostaglandin promotion of osteocyte gap junction function through transcriptional regulation of connexin 43 by glycogen synthase kinase 3/beta-catenin signaling. Mol Cell Biol 2010; 30: 206–219
41. Cherian PP, Cheng B, Gu S *et al.* Effects of mechanical strain on the function of Gap junctions in osteocytes are mediated through the prostaglandin EP2 receptor. J Biol Chem 2003; 278: 43146–43156
42. Cheng B, Kato Y, Zhao S *et al.* PGE(2) is essential for gap junction-mediated intercellular communication between osteocyte-like MLO-Y4 cells in response to mechanical strain. Endocrinology 2001; 142: 3464–3473

Received for publication: 31.3.2013; Accepted in revised form: 3.8.2013